EUROFUSION WPMST1-PR(16) 16356

CJ Rapson et al.

Improved localisation of Neoclassical Tearing Modes by combining multiple diagnostic estimates.

Preprint of Paper to be submitted for publication in
Nuclear Fusion

This work has been carried out within the framework of the EUROfusion Consortium and has received funding from the Euratom research and training programme 2014-2018 under grant agreement No 633053. The views and opinions expressed herein do not necessarily reflect those of the European Commission.

Improved localisation of Neoclassical Tearing Modes by combining multiple diagnostic estimates.

C J Rapson[1], R Fischer, L Giannone[1], M Maraschek[1], M Reich[1], W Treutterer[1] and the ASDEX Upgrade Team[1]

1 Max Planck Institute for Plasma Physics, Boltzmannstrasse 2, 85748 Garching, Germany

E-mail: chris.rapson@ipp.mpg.de

Abstract. Neoclassical Tearing Modes (NTMs) strongly degrade confinement in tokamaks, and are a leading cause of disruptions. They can be stabilised by targetted Electron Cyclotron Current Drive (ECCD), however the effectiveness of ECCD depends strongly on the accuracy or misalignment between ECCD and the NTM. The first step to ensure minimal misalignment is a good estimate of the NTM location. In previous NTM control experiments, three methods have been used independently to estimate the NTM location: the magnetic equilibrium, correlation between magnetic and spatially-resolved temperature fluctuations, and the amplitude response of the NTM to nearby ECCD. This submission describes an algorithm which has been designed to fuse these three estimates into one, taking into account many of the characteristics of each diagnostic. Although the method diverges from standard data fusion methods, results from simulation and experiment confirm that the algorithm achieves its stated goal of providing an estimate that is more reliable and accurate than any of the individual estimates.

PACS numbers: 52.55.Fa

Keywords NTM, data fusion, real-time diagnostics Submitted to: *Nucl. Fusion ?*

1. Introduction

Neoclassical Tearing Modes (NTMs) degrade confinement in tokamaks and cause disruptions e.g. [1]. NTMs can be controlled by depositing Electron Cyclotron Current Drive (ECCD) but the power requirements are extremely sensitive to the accuracy of the deposition with respect to the NTM. For a misalignment as small as 1.5 cm at ASDEX Upgrade (AUG) no amount of power will shrink the NTM island below its marginal width [2]. For ITER, similar values in the range of $1-2$ cm are predicted [3].

New experimental results indicate that the accuracy requirements can be relaxed if the ECCD is swept repeatedly across the island [4]. The strategy is that the ECCD beam will definitely be inside the island at some point during the sweep, and that the time spent misaligned does not destabilise the island. It is, however, a sub-optimal use of ECCD power. The amplitude of the sweep is driven by the uncertainty of the estimate of the NTM location, therefore a more accurate estimate would reduce the sweep amplitude and hence reduce both the wasted power and the time required to stabilise the NTM.

The location of the NTM has been estimated in previous experiments using three different methods. Firstly, reconstruction of the safety factor (q) profile gives a position for the rational surfaces where NTMs occur - usually $q = 1.5$ or $q = 2.0$. The advantage of this method is that the q-profile can be estimated before an NTM appears, and hence can be used for pre-emptive NTM control [5–7]. The disadvantage is that accurate real-time measurements of the internal q-profile are difficult, so the estimates have a large uncertainty. Secondly, by correlating fluctuations in Electron Cyclotron Emissions (ECE) with magnetic field fluctuations measured by Mirnov coils, it is possible to identify the ECE channel which is closest to the centre of the NTM [8]. At low NTM amplitudes, the signal-to-noise ratio of this method can be poor, which leads to some degree of false localisations. In addition, the ECE measurements are sometimes disturbed in the vicinity of strong ECCD - which is precisely the case when stabilising an NTM.

Previous work attempted to combine these first two methods into a single estimate of the NTM location [9], however the project was discontinued due to a lack of manpower before it could achieve satisfactory results, and was never deployed on the real-time control system.

Both the equilibrium and the ECE correlation estimate the NTM position in terms of the normalised magnetic flux co-ordinate ρ_{pol}. For control, the ECCD is controlled using front-steering mirrors and the deposition location is estimated using real-time ray tracing [10]. Ray-tracing introduces a dependency on the density profile and means that the uncertainty of the equilibrium reconstruction also applies to the ECE correlation estimate - if only in terms of shape, not in terms of absolute q-values.

The third method estimates the NTM location by measuring changes in the island size via the amplitude of the signal from the Mirnov coils. Various forms of extremum controllers have been developed to position the ECCD steering mirrors so as to minimise

the Mirnov coils' signal amplitude. Variations on the extremum controller include sweeping and detecting the minimum amplitude [11, 12] or searching in steps for an incrementally better alignment [11, 12] or building up an estimate by comparing the measurements with a model of expected NTM behaviour [11,13]. It is however not trivial to design an extremum (i.e. non-linear) controller for a noisy environment, and Mirnov coil signals are notoriously noisy. In fact, the noise level on these signals makes it difficult to even reliably detect whether an NTM is present or not, especially in scenarios with other MHD activity such as ELMs, fishbones or sawteeth. For differentiating between different modes, a singular value decomposition method using many coils is a more robust alternative [14]. The disadvantage for methods using either the NTM amplitude or the ECE correlation is that an NTM must appear before it can be localised, so these methods are not suitable for pre-emptive control.

Fortunately, many of the advantages and disadvantages of these three methods are complementary, and so this problem is well suited for combining their estimates to produce an output which is better than any of the inputs by itself. This process is known as data fusion e.g. [15]. There is extensive literature on various techniques which can be applied depending on the system. In general, data fusion of plasma diagnostics has immense potential, both for offline analyis e.g. [16] and for real-time control e.g. [17, 18]. With a relatively small effort, plasma parameters can be estimated with smaller error bars and improved robustness to diagnostic failure. Certainly, for larger fusion devices with correspondingly higher reliability requirements, data fusion should become an essential part of the real-time control system.

2. Algorithm Design

2.1. Choice of Algorithm Type

In order to choose the most appropriate data fusion method, the characteristics of the individual estimates and the dynamics of the NTM have been analysed. Both the estimate from the equilibrium reconstruction and from the ECE correlation can be modelled as Gaussian probability density functions (PDFs) with a prescribed variance. The estimate of the location based on the amplitude is however multimodal, since for multiple ECCD beams, it is not possible to know which one was responsible for the change in the NTM amplitude, based on a single measurement. This rules out many of the simpler methods such as a linear Kalman filter, or even the approximately linear variants, since a multimodal distribution can not be easily linearised.

The proposed model of the NTM location dynamics is very simple, where its location at the next timestep is its location from the previous timestep, with some uncertainty referred to as "process noise". However, NTMs have the tendency to appear and disappear (with or without active stabilisation) [1]. They may even re-appear in a different location if the q-profile has changed in the meantime. Particle filters are a common technique for non-linear parameter estimation problems, but sample degeneracy

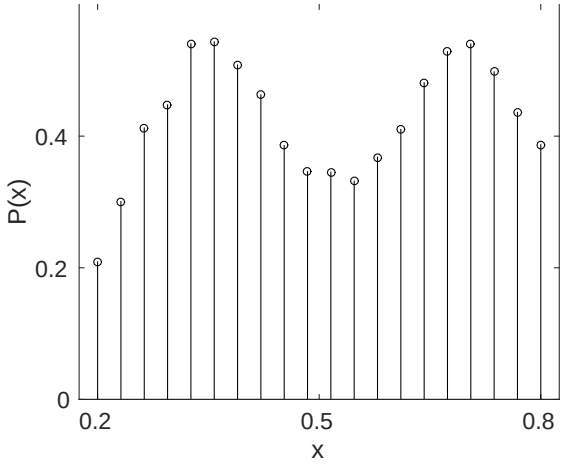

Figure 1. A schematic of a bimodal PDF with some noise discretised on a grid. The grid points are fixed and regular, whereas for a particle filter the resampling process would tend to bunch points around regions with higher prior probability.

could lead to having no particles in the region where a new NTM is born, and hence being unable to localise it. This is a known problem observed with e.g. occlusion in tracking of objects from video analysis e.g. [19]. Therefore, a similar method without resampling was chosen - a 1-dimensional grid filter [20]. Fig. 1 shows a sketch of how a bimodal PDF could be represented by a grid filter. The grid points are fixed, and the probability density at each point evolves in time by alternately incorporating information from measurements and the model of NTM location dynamics.

In order to avoid calculating the PDF for the linear equilibrium and ECE estimates across the full grid, these are treated as Gaussian and tracked as a mean and covariance. The prediction step consists of updating the covariance by adding process noise of $10s^{-1}$ in ρ_{pol}. At each time step a Gaussian is calculated from these parameters to be combined with the non-linear amplitude based estimate. Since the amplitude estimate has no concept of covariance, the update would normally be done by simulating a Markov chain for each point in the grid. However, here a simpler method was chosen which will be described in section 2.2.

2.2. Location Estimate from NTM Amplitude

It was noted already that the amplitude based estimate of the NTM location is a multimodal PDF. However this is not the only complication when designing the observation model. A decrease of the NTM amplitude implies that at least one ECCD beam is on target, which can be represented by the PDF in fig. 2 a). It is however not obvious how to handle the case where the NTM amplitude increases. For a noisy signal such as NTM amplitude, an increase and decrease of equal magnitude should cancel each other out. Hence, taking the inverse PDF or calculating $(2 * max(PDF) - PDF)$ as shown in fig. 2 b) and fig. 2 c) respectively, are not good representations. Therefore it was decided to try simply taking the negative of the PDF for increasing NTM amplitudes

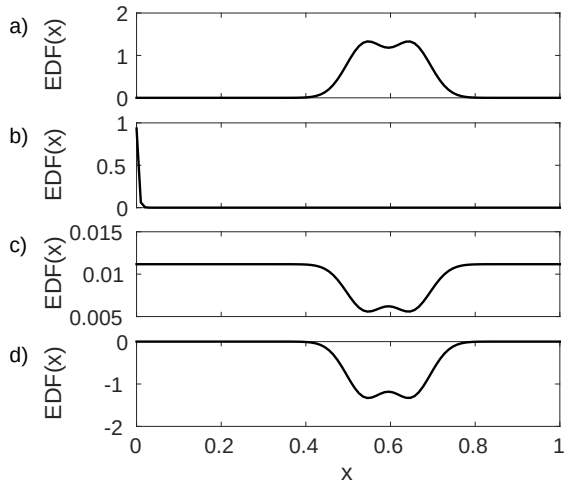

Figure 2. Some example Expectation Density Functions representing the expectation $EDF(x)$ of the NTM being at a location x. Frame (a) for ECCD at $x = 0.54$ and $x = 0.65$ and decreasing NTM amplitude indicating that one or both are on target. Frame (b) is the inverse of frame (a), rescaled so that the integral is 1. Frame (c) is $2 * max(EDF(x)) - EDF(x)$, rescaled so that the total probability is 1. Frame (d) is the negative of frame (a).

and a positive PDF for decreasing amplitudes. Of course, negative distributions do not correspond to a "probability density" so these will be referred to as "expectation distribution functions" (EDF). In addition, this prevents the use of Bayesian logic to combine estimates. Instead, it was decided to add EDFs from each of the three estimates. Since a Markov chain is no longer applicable for the prediction step, a simple exponential forgetting factor was used so that information value decays towards zero over time, whether it is positive or negative. The choice for the time constant was driven mostly by the dynamics of the mirrors. Sweeping around the estimated NTM location is limited to 3 Hz, so a value of 0.7 s ensures that information from the previous sweep is not completely forgotten before the mirror returns to a given location.

Despite the obvious drawbacks of using negative distributions, good results were achieved quickly, which motivated continuing with this unconventional approach. In all likelihood, equivalent or better results could be achieved using a formal Bayesian method. Nevertheless, this paper describes the chosen method, which is justified pragmatically through the short deployment time and empirically observed accuracy and robustness.

2.3. Uncertainties and Weightings

The uncertainty for the equilibrium reconstruction was set based on prior experience to be a variance of 0.02 in ρ_{pol}.

The uncertainty for the ECE correlation is limited by the spacing between ECE channels, and in addition is larger if the NTM is smaller. The variance is calculated for

each timestep as

$$var_{ECE} = 0.004 \left(\frac{NTM\ detection\ threshold}{NTM\ amplitude} \right)^2 \quad (1)$$

The amplitude has been median filtered over 25 samples (approximately 40ms) to remove spikes from ELMs.

The estimate based on changes in the NTM amplitude has more dependencies, and this is reflected in a relatively complex combination of weightings which are used to calculate the EDF. Each ECCD beam which is within 0.1 in ρ_{pol} contributes a Gaussian peak to the estimate, originally with a variance set to 0.004. The contribution of beams is then weighted with the power as a fraction of the total "on target" power. After combining the contribution for each beam, the full EDF is weighted by the magnitude of the change in NTM amplitude, normalised to the average magnitude of the change in NTM amplitude so far for the running shot. Finally, the EDF was weighted again by changes in the ratio of plasma pressure to the poloidal magnetic field (β_{pol}). Since NTMs are pressure driven instabilities, the amplitude reacts to changes in the pressure, which could be misinterpreted as an indication that ECCD is on or off target. As an equation, the EDF for the amplitude based estimate is given by:

$$EDF_{ampl} = \left(\left(\frac{d\ \beta_{pol}}{d\ t} \right)^2 + 1 \right) \frac{\frac{-d\ ampl}{d\ t}}{\left\langle \frac{d\ ampl}{d\ t} \right\rangle} \sum_{i=1}^{i=n_{gyr}} \frac{P_{ECCD,i}}{\Sigma P_{ECCD}} exp \left(-\frac{\left(\rho - \rho_{ECCD,i}\right)^2}{0.004} \right) \quad (2)$$

Where the number of gyrotrons near the previous estimate is n_{gyr} and angle brackets indicate averaging over time between the start of the shot and the latest measurement.

When adding EDFs from the three estimates, a final weighting factor was used to empirically adjust the trust in each measurement. The weighting factors proved to be a useful tuning knob both in the offline simulations and the experiment. After some testing, it was decided to weight the equilibrium and ECE correlation estimates equally with 1, while the amplitude based estimate was weighted with 0.012 to compensate for the integrating effect of the forgetting factor.

3. Simulation Results

The design was verified in simulation before being deployed on the real-time control system. Firstly, using diagnostic data from previous shots, and then with full closed loop feedback.

3.1. Simulation Results with Input from Archived Data

53 shots with NTMs were tested to ensure the robustness of the algorithm. Fig. 3 shows the results for #30594, a shot which has been studied in some detail [4, 21, 22]. Note that the equilibrium estimate in frame (c) has a constant spread which is relatively wide and has a lower maximum than the others. Therefore the equilibrium generally has less

influence on the final estimate. The exception is at the start of the discharge, since before the NTM appears, the equilibrium is the only viable estimate.

In contrast, the spread (and hence the highest point) of the ECE correlation estimate depends on the NTM amplitude, giving a narrow EDF from $t = 2.1..2.4\,\mathrm{s}$. The spread in the location estimate for small NTMs can be seen in frame (a) at the beginning ($t < 2.1\,\mathrm{s}$) and end of the shot ($t > 6.0\,\mathrm{s}$). The amplitude based EDF is zeroed until ECCD is switched on and close to the estimated NTM location. Even if the ECCD were switched on, the large drop in NTM amplitude at $t = 2.4\,\mathrm{s}$ would be ignored since this is related to a drop in β as the NBI beams are switched off. As the ECCD beam sweeps across the NTM, note the amplitude reduction near the outside of the sweep (high ρ_{pol}) and the amplitude recovery when ECCD is deposited off target. The amplitude EDF is positive when the amplitude shrinks, and negative when it grows, leading to a strong indication that the true NTM location is just inside the outer limit of the sweep. In frame (a), note how the combined estimate is shifted gradually outwards from the ECE correlation estimate, from $t = 4\,\mathrm{s}$ onwards. This timing corresponds to the start of a second gyrotron, which causes stronger changes in the NTM amplitude.

Most importantly, it can be seen from fig. 3 that the algorithm combines the strengths of the three estimates, so that in each phase of the discharge, the final estimate is dominated by the most appropriate diagnostic method. The exception to this is around $t = 2\,\mathrm{s}$, where the NTM has started growing, but the ECE correlation with the more central m/n=1/1 mode is still stronger than with the 3/2 NTM, thus giving an incorrect estimate which is interpreted as having a high degree of confidence. It is unclear at this stage how this could be improved upon.

3.2. Simulation Results with a Formal Bayesian Approach

Simulations were attempted using proper PDFs ($\int P(x)dx = 1,\ P(x) > 0\ \forall x$) using the distribution from fig. 2 c) whenever the NTM amplitude increases. The result is shown in fig. 4 where despite several attempts at tuning the free parameters, the result is not as satisfactory (subjectively) as the result using a negative distribution function. The information from the rising NTM amplitude (i.e. where the ECCD beam is poorly aligned) seem to have only a small influence on the final estimate, which undervalues this source of information.

3.3. Simulation Results with Feedback

Full feedback simulations provided further confidence in the robustness of the algorithm, and its ability to quickly stabilise an NTM. The simulation models the dynamics of the control system and the steering mirrors [23] and a Modified Rutherford Equation [2] to model the NTM evolution. Fig. 5 shows a result using the equilibrium reconstruction and ECE correlation estimates from #30057. The "true NTM location" was generated by a random deviation from the equilibrium $q = 1.5$ surface, which was then low-pass filtered. Once again, the combined estimate matches the equilibrium estimate until the

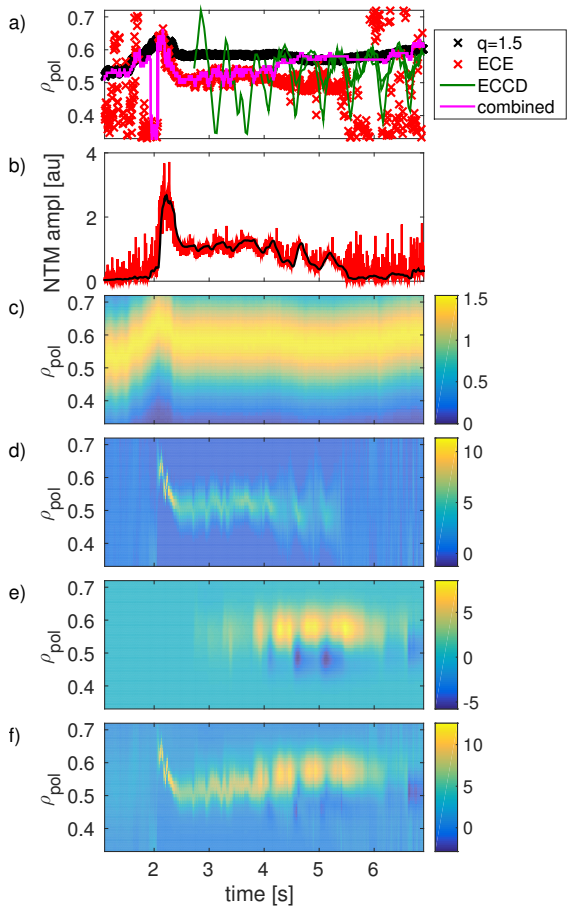

Figure 3. A simulation result using archived measurement data as input to the data fusion algorithm. Frame (a) shows the raw localisation from the $q = 1.5$ surface from the equilibrium (x), along with the estimate from ECE correlation (x) and the ECCD deposition locations (-). In magenta is the combined estimate as output by the algorithm (-). Frame (b) shows the NTM amplitude as the envelope of the magnetic field fluctuations measured by Mirnov coils, with the raw measurement in red and the median filtered version in black. Frame (c) shows the time dependent EDF for the equilibrium estimate. Similarly for frame (d) with the ECE correlation estimate, as well as frame (e) with the amplitude based estimate, which has been weighted by a factor of 0.012. Frame (f) shows the combined EDFs resulting from adding the individual EDFs.

NTM is triggered at $t = 1.7\,\mathrm{s}$. At this point the estimate tracks the ECE correlation estimate until ECCD is switched on. As the island shrinks, the amplitude based estimate becomes ever more confident until the NTM is stabilised. From the feedback simulation it was found that sweeping the mirrors is highly beneficial, since this provides fresh input to the amplitude based estimate. Without sweeping, the estimate may become locked in a local minimum.

The sweep is made about the point of maximum likelihood, down to the first point on either side which has $< 90\%$ of this maximum likelihood. Therefore, EDFs with a large uncertainty will have a large sweep to ensure that the island really will be crossed.

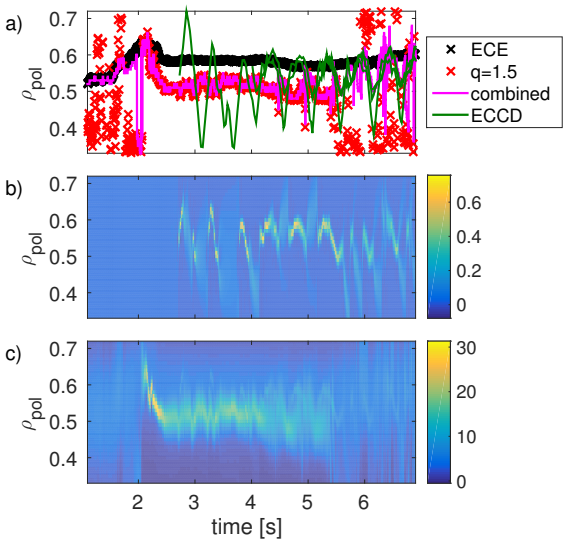

Figure 4. A simulation result using proper PDFs combined using Bayesian logic. Frame (a) is as for fig. 3. Frame (b) is the amplitude based estimate and frame (c) shows the combined PDF. The combined PDF is calculated for each time step by multiplying the prior by each of the estimates in turn and normalising to give an integral of 1. The PDFs from equilibrium and ECE correlation are not shown, as they are identical to those in fig. 3.

As the estimate becomes more confident, the sweep becomes smaller.

4. Experimental Results

During the recent AUG campaign, a small number of shots were run using the new algorithm for feedback NTM control. During the weeks where these shots were run there was unfortunately a problem with the real-time ECE correlation, so that the algorithm first had to demonstrate a robustness to a corrupt input. Using the so-called quality tags prescribed by the Discharge Control System (DCS) [24], this input was recognised as corrupt and the estimate was constructed by combining the remaining two inputs.

Fig. 6 shows the localisation of a 2/1 NTM in #33114. During this and other shots, an unexpected coupling between the NTM localisation and the ECCD power controller was observed. The feedback simulations referred to in section 3.3 considered only the control of the mirror movement, and assumed that the ECCD power was constantly on. When the ECCD power is feedback controlled, it is only switched on when ray tracing indicates that the deposition would be close to the target. Here, power is switched on at $t = 2.99\,\mathrm{s}$, which considerably slows the growth rate of the NTM, but does not manage to shrink it with only 600 kW. Since the NTM is still slowly growing, the algorithm deduces that the ECCD must be at the wrong place, and shifts the target quite dramatically outwards by 0.05 in ρ_{pol}. Now the deposition location is outside the light band in fig 6 a), and the power is switched off. If the power remained on, the

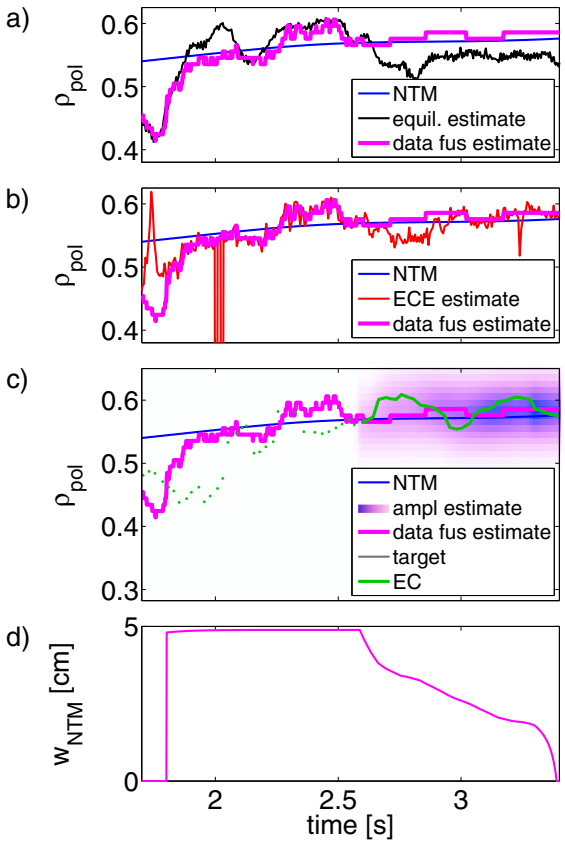

Figure 5. A result from a simulation modelling a closed feedback loop. The "true" NTM location in blue and the combined estimate in magenta appear in frames (a),(b) and (c). In frame (a) they are compared to the estimate from the equilibrium reconstruction. Frame (b) shows the estimate from ECE correlation and frame (c) shows the EDF from the amplitude based estimate in purple, along with the ECCD deposition location in green. Green dots show where the deposition would have been at times where the EC power was off. Frame (d) shows the simulated NTM amplitude.

localisation algorithm would have a chance to correct its mistake. However, in this case the error is preserved until the mirrors move such that the deposition is close to the NTM location again at $t = 3.11\,\mathrm{s}$. Unfortunately, the mirror motion is now out of phase with the sweeping trajectory. Due to their inertia, they overshoot and the power is switched off again.

To combat this problem, the weighting for the amplitude based estiamte was reduced from 0.012 to 0.006 and the ECCD power controller was made more tolerant - keeping the power on until the misalignment in ρ_{pol} exceeds 0.1 instead of 0.05.

Note that while all other examples shown are for 3/2 NTMs, #33114 had a 2/1 NTM. By duplicating the algorithm and running two versions with different input signals, the location of both NTM modes are estimated in parallel.

In #33642 the improvements seem to have worked, as shown in fig. 7. Despite strong fluctuations in β due to pulse width modulation of an NBI beam, the NTM is well localised and appears to be on its way to being stabilised with just 600kW of

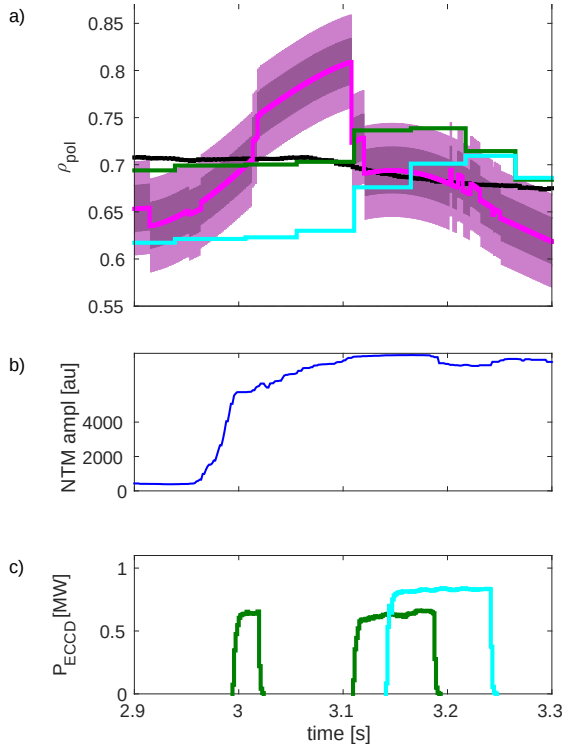

Figure 6. A short excerpt from shot #33114 showing in frame (a) the $q = 2.0$ surface in black (-) along with a target sweeping around the combined estimate in magenta (-). The shaded regions show the tolerable difference around the estimated NTM location within which the ECCD power will be switched on (darker) and switched off (lighter). The deposition locations for two gyrotrons are shown in green (-) and cyan (-). Frame (b) shows the amplitude of the 2/1 NTM and frame (c) shows the ECCD power of the two gyrotrons, with colours corresponding to their deposition locations.

ECCD power in a plasma with $\beta_N \approx 3.0$. (The shot came to a planned end while the NTM amplitude was still decreasing.) This efficiency implies that the ECCD was accurately deposited within the NTM island. The excursions of the NTM location estimate are much smaller than for #33114 and the gyrotrons that switch off do so because of tripping, not because of the controller. The amplitude of the sweeping can be seen to decrease with increasing time, indicating that the uncertainty of the estimate of the NTM location was decreasing from the beginning (using only the $q = 1.5$ surface) to the end.

5. Conclusions

An algorithm has been developed which combines three different estimates of the NTM location to produce a combined estimate which is more robust and accurate than any of the inputs by themselves. The inputs are 1) the rational q-surfaces from the equilibrium reconstruction, 2) the ECE channel location selected using correlation with magnetic fluctuation signals from Mirnov coils, and 3) interpreting the change in the NTM amplitude as an indication of the accuracy (or misalignment) with which ECCD is

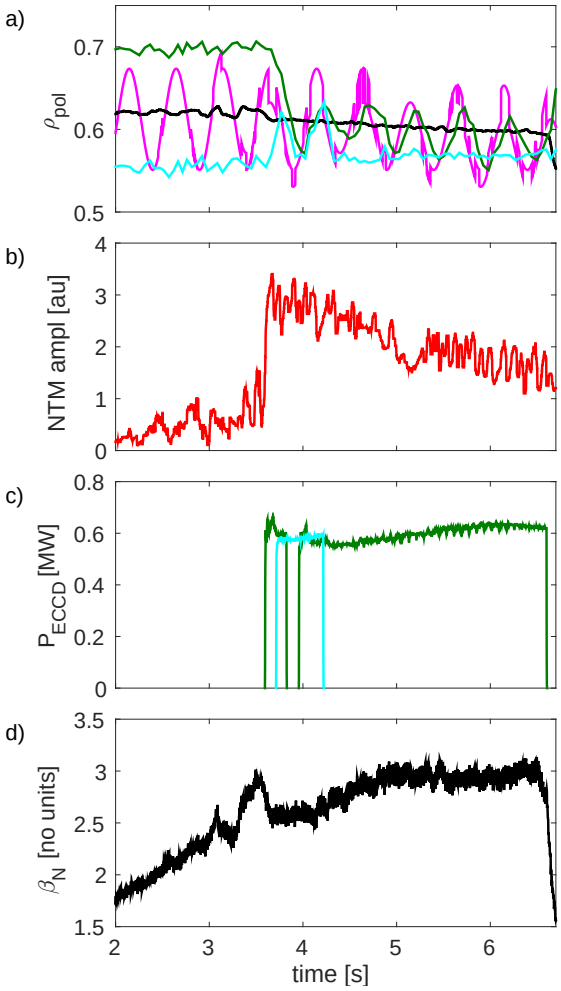

Figure 7. Localisation of a NTM using the data fusion algorithm in a feedback control experiment. Frame (a) shows the $q = 1.5$ surface from the equilibrium reconstruction in black (-), with the target sweeping around a combined estimate in magenta (-). The green (-) and cyan (-) lines show the deposition location of two ECCD beams. Frame (b) shows the NTM amplitude. ECE localisation was not available in real-time (so is not shown here). Frame (c) shows the ECCD power with colours corresponding to the same gyrotrons as in frame (a). Frame (d) shows the normalised plasma pressure.

tracking the NTM. The algorithm takes into account many features of each diagnostic, for instance the uncertainty, which may be parameterised to reflect dependencies on the island size in the case of the ECE correlation, or on changes in β for the amplitude based estimate.

The choice of method to combine the estimates was driven by the characteristics of the diagnostics. A grid based filter was determined to be more appropriate than any of the Kalman filter variants or a particle filter. For pragmatic reasons, it was decided to depart from conventional PDFs and Bayesian logic. This decision is justified to some extent by the good results achieved with the unconventional method, although it would be interesting to see if these results can be matched or improved upon by developing a

more conventional method in the future.

Data fusion is an extremely useful and underutilised tool for estimating plasma parameters from uncertain, noisy and potentially even malfunctioning diagnostic measurements - both offline and in real-time. Improvements in the individual diagnostics are important, but given the stringent requirements for NTM localisation, none of the methods seems to be sufficient by itself. The synergies of the diagnostics' respective advantages and disadvantages make NTM control significantly more accurate and robust when they are fused. If NTMs can be reliably stabilised, high levels of confinement can be maintained and a proportion of disruptions can be avoided.

6. Acknowledgements

This work has been carried out within the framework of the EUROfusion Consortium and has received funding from the Euratom research and training programme 2014-2018 under grant agreement No 633053. The views and opinions expressed herein do not necessarily reflect those of the European Commission.

References

[1] Maraschek M 2012 *Nucl. Fusion* **52** 074007 URL http://stacks.iop.org/0029-5515/52/i=7/a=074007

[2] Urso L 2009 *Modelling and Experiments on NTM stabilisation at ASDEX Upgrade* Ph.D. thesis Technische Universitaet Muenchen

[3] La Haye R J 2015 *AIP Conf. Proc.* **1689** 030018 URL http://scitation.aip.org/content/aip/proceeding/aipcp/10.1063/1.4936483

[4] Reich M, Barrera L, Behler K, Buhler A, Bock A, Eixenberger H, Fietz S, Fischer R, Giannone L, Lackner K, Lochbrunner M, Maraschek M, McCarthy P, Monaco F, Mlynek A, Poli E, Preuss R, Rapson C J, Sauter O, Schubert M, Stober J, Treutterer W, Volpe F, Wagner D, Zohm H and ASDEX Upgrade team 2014 Real-time control of NTMs using ECCD at ASDEX Upgrade *Submitted to Proceedings of the 25th IAEA Fusion Energy Conference, St. Petersburg, Russia* URL https://conferences.iaea.org/indico/contributionDisplay.py?contribId=430&sessionId=27&confId=46

[5] La Haye R J 2006 *Phys. Plasmas* **13** ISSN 1070-664X 47th Annual Meeting of the Division of Plasma Physics of the American-Physical-Society, Denver, CO, OCT 24-28, 2005

[6] Giannone L, Reich M, Maraschek M, Poli E, Rapson C, Barrera L, McDermott R, Mlynek A, Ruan Q, Treutterer W, Wenzel L, Bock A, Conway G, Fischer R, Fuchs J, Lackner K, McCarthy P, Preuss R, Rampp M, Schuhbeck K, Stober J and Zohm H 2013 *Fusion Eng. Des.* **88** 3299 – 3311 ISSN 0920-3796 URL http://www.sciencedirect.com/science/article/pii/S0920379613006844

[7] Kolemen E, Welander A, Haye R L, Eidietis N, Humphreys D, Lohr J, Noraky V, Penaflor B, Prater R and Turco F 2014 *Nucl. Fusion* **54** 073020 URL http://stacks.iop.org/0029-5515/54/i=7/a=073020

[8] Reich M, Bock A, Maraschek M and ASDEX Upgrade Team 2012 *Fusion Sci. Technol.* **61** 309–313 ISSN 1536-1055

[9] Manini A, Berrino J, Cirant S, D'Antona G, Gandini F, Grnwald G, Leuterer F, Maraschek M, Monaco F, Neu G, Raupp G, Sormani D, Stober J, Suttrop W, Treutterer W, Wagner D and Zohm H 2007 *Fusion Eng. Des.* **82** 995–1001 cited By (since 1996):19 URL www.scopus.com

[10] Reich M, Bilato R, Mszanowski U, Poli E, Rapson C, Stober J, Volpe F and Zille R 2015 *Fusion Engineering and Design* **100** 73 – 80 ISSN 0920-3796 URL http://www.sciencedirect.com/science/article/pii/S0920379615002537

[11] Humphreys D, Ferron J, La Haye R, Luce T, Petty C, Prater R and Welander A 2006 *Phys. Plasmas* **13** 056113 (9pp) ISSN 1070-664X 47th Annual Meeting of the Division of Plasma Physics of the American-Physical-Society, Denver, CO, OCT 24-28, 2005

[12] Rapson C, Giannone L, Maraschek M, Reich M, Stober J and Treutterer W 2014 *Fusion Eng. Des.* **89** 568 – 571 ISSN 0920-3796 Proceedings of the 9th IAEA Technical Meeting on Control, Data Acquisition, and Remote Participation for Fusion Research URL http://www.sciencedirect.com/science/article/pii/S0920379614000088

[13] Wehner W and Schuster E 2012 *Nucl. Fusion* **52** 074003 URL http://stacks.iop.org/0029-5515/52/i=7/a=074003

[14] Galperti C, Marchetto C, Alessi E, Minelli D, Mosconi M, Belli F, Boncagni L, Botrugno A, Buratti P, Calabro' G, Esposito B, Garavaglia S, Granucci G, Grosso A, Mellera V, Moro A, Piergotti V, Pucella G, Ramogida G, Bin W and Sozzi C 2014 *Plasma Phys. Contr. Fusion* **56** 114012 URL http://stacks.iop.org/0741-3335/56/i=11/a=114012

[15] Mitchell H 2007 *Multi-Sensor Data Fusion: An Introduction* (Springer) ISBN 9783540715597 URL https://books.google.de/books?id=2hwcFSxQ1CAC

[16] Fischer R, Fuchs C J, Kurzan B, Suttrop W, Wolfrum E and ASDEX Upgrade Team 2010 *Fusion Sci. Technol.* **58** 675–684 ISSN 1536-1055

[17] Felici F, Rapson C, Treutterer W, Giannone L, Maljaars E, van den Brand H, Reich M, Sauter O, Teplukhina A, Kim D, Piovesan P, Piron C, Barrera L, Willensdorfer M, Bock A, Fable E, Geiger B, Tardini G and the ASDEX-Upgrade team 2015 Real-time plasma profile state reconstruction on ASDEX-Upgrade *Europhysics Conference Abstracts, Proceedings of the 42nd EPS Plasma Physics Conference, Lisbon (2015) Paper O4.127* p O4.127 URL http://ocs.ciemat.es/EPS2015ABS/pdf/O4.127.pdf

[18] Blanken T, Felici F, Rapson C, the TCV team and the ASDEX-Upgrade team 2016 Particle density modeling for density profile reconstruction and fringe jump detection on TCV and ASDEX Upgrade *43rd European Physical Society Conference on Plasma Physics (EPS), Leuven, Belgium, 4th July 2016.* P4.031 URL http://ocs.ciemat.es/EPS2016PAP/pdf/P4.031.pdf

[19] Herrmann M, Hoernig M and Radig B 2014 {*AASRI*} *Procedia* **8** 30 – 37 ISSN 2212-6716 2014 {AASRI} Conference on Sports Engineering and Computer Science (SECS 2014) URL http://www.sciencedirect.com/science/article/pii/S2212671614000730

[20] Alin A, Butz M V and Fritsch J 2011 Tracking moving vehicles using an advanced grid-based Bayesian filter approach *2011 IEEE Intelligent Vehicles Symposium (IV) Baden-Baden, Germany, June 5-9, 2011* URL http://ieeexplore.ieee.org/stamp/stamp.jsp?arnumber=5940471

[21] Maraschek M, Reich M, Behler K, Giannone L, Poli E, Rapson C, Sauter O, Stober J, Treutterer W, Zohm H and ASDEX Upgrade team 2015 Real-time control of MHD instabilities using ECCD in ASDEX Upgrade *Europhysics Conference Abstracts, Proceedings of the 42nd EPS Plasma Physics Conference, Lisbon (2015) Paper 1.112* p P1.112 URL http://ocs.ciemat.es/EPS2015ABS/pdf/P1.112.pdf

[22] Février O, Maget P, Ltjens H, Giruzzi G, Reich M, Sauter O, Beyer P, the ASDEX Upgrade team and the EUROfusion MST1 Team 2015 Modeling of the impact of ECCD sweeping on NTM stability in ASDEX-Upgrade *Europhysics Conference Abstracts, Proceedings of the 42nd EPS Plasma Physics Conference, Lisbon (2015) Paper P1.104* p P1.104 URL http://ocs.ciemat.es/EPS2015ABS/pdf/P1.104.pdf

[23] Rapson C, Monaco F, Reich M, Stober J, Treutterer W and the ASDEX Upgrade Team 2013 *Fusion Eng. Des.* **88** 1137 – 1140 ISSN 0920-3796 proceedings of the 27th Symposium On Fusion Technology (SOFT-27); Liége, Belgium, September 24-28, 2012 URL http://www.sciencedirect.com/science/article/pii/S0920379613002421

[24] Treutterer W, Cole R, Lueddecke K, Neu G, Rapson C, Raupp G, Zasche D and Zehetbauer T 2014 *Fusion Eng. Des.* **89** 146 – 154 ISSN 0920-3796 design and implementation of real-time systems for magnetic confined fusion devices URL `http://www.sciencedirect.com/science/article/pii/S0920379614000027`